



# Influence of liquid nitrogen cooling on the spectral performance of BAC-P in bismuth-doped phosphosilicate fibers under liquid nitrogen temperature

QIANCHENG ZHAO,<sup>1</sup> , QUN HAO,<sup>2,\*</sup> , CHANGYUAN YU,<sup>3</sup> FENGZE TAN,<sup>3</sup> YANHUA LUO,<sup>1</sup> AND GANG-DING PENG<sup>1</sup>

<sup>1</sup>Photonics and Optical Communications Group, School of Electrical Engineering, University of New South Wales, Sydney, NSW 2052, Australia

<sup>2</sup>School of Optics and Photonics, Beijing Institute of Technology, Beijing 100081, China

<sup>3</sup>Photonics Research Center, Department of Electronic and Information Engineering, The Hong Kong Polytechnic University, Hong Kong, China

\*qhao@bit.edu.cn

**Abstract:** The first results of the liquid nitrogen cooling effect on the spectral properties of a phosphor-related bismuth active center (BAC-P) have been presented. It is found that the small-signal absorption bands of BACs are mildly affected at liquid nitrogen temperature (LNT, 77 K), while the unsaturable absorption level is lowered moderately. Meanwhile, noticeable shape changes of luminescence spectra and enhanced luminescence intensity ( $\sim$  twice) of BAC bands were revealed at LNT upon excitation at 830 or 980 nm, which is contributed by the notable growth of BAC-P. In addition, the influence of cooling on the on-off gain performance of BACs is also explored. Furthermore, the laser-induced effect on the luminescence of BAC-P upon cooling at LNT is also investigated, revealing a noticeable increase ( $\sim$ 10%) instead of photobleaching. These experimental results bring new insights into the temperature-related spectral properties of BACs and provide an effective way for tuning the luminescence scheme for Bi-doped fibers by cryogenics for the desired spectral range 1.26–1.36  $\mu$ m.

© 2020 Optical Society of America under the terms of the [OSA Open Access Publishing Agreement](#)

## 1. Introduction

Since the first demonstration of Nd-doped glass fiber laser in the 1960s [1], great attention has been paid to the search for new active laser media. Bismuth (Bi)-doped fibers (BDF), as a promising gain medium, have been intensively explored for their broadband luminescence, gain, and lasing in the spectral range 1.15–1.5  $\mu$ m and 1.6–1.8  $\mu$ m, where no efficient rare-earth-doped fiber lasers exist [2–4]. To further extend the operating wavelength range, Bi-doped fibers with rare-earth elements (e.g. erbium, ytterbium) have been intensively fabricated by National Fiber Facility at UNSW. Excitingly, ultra-broadband luminescence spreading from 1 to 1.7  $\mu$ m has been achieved in a single Bi/Er/Yb codoped fiber (BEYDF) upon excitation at 830 nm [5]. Moreover, broadband on-off gain over 2.4 dB/m in the spectral range 1.3–1.6  $\mu$ m has also been obtained in the Bi/Er codoped silicate fiber (BEDF) with only one pump source at 830 nm [6]. The notable progress in Bi-doped devices has found widespread use in optical communication, medicine, material treating, and sensing. However, despite the success in this realm, it turns out that the nature of bismuth NIR emitting centers remains disputable. Currently, the efficient operation of Bi-doped fiber lasers can only be achieved with a low doping level of bismuth ( $\leq$  0.1 wt.%) [7,8]. Therefore, various post-treatments (e.g., ionizing irradiation [9–11], hydrogen loading [12,13]) have been attempted to improve the spectral performance of BDFs. Specifically, thermal treatment upon heating at high temperatures is found to be an effective approach for the activation of BACs (BAC-Si and BAC-Ge) [14,15]. Nevertheless, all current thermal studies involve a

heating process in the high-temperature range (up to several hundred degrees centigrade) with subsequent cooling at different rates [14–16]. Whereas the study of the effect of direct cooling in the low-temperature zone on the spectral properties of BDFs is very limited, which may shed some light on the structure of Bi-related luminescence centers. Specifically, the spectral region of 1.26–1.36  $\mu\text{m}$  (O-band) is of special interest due to the near-zero dispersion and low transmission loss attained in single-mode fibers, and bright luminescence in this range has been observed in BDFs with the  $\text{SiO}_2\text{-P}_2\text{O}_5$  host.

Therefore, in this paper, to further enhance the understanding the effect of cooling on the spectral properties of BAC-P in Bi-doped phosphosilicate fibers, a series of optical experiments have been carried out to systematically characterize the spectral absorption, luminescence, on-off gain, and photo-induced properties of BAC-P at both room temperature (RT, 25  $^\circ\text{C}$ ) and LNT ( $-196$   $^\circ\text{C}$ ). These experimental data provide new information on the temperature-related spectral properties of BAC-P and provides a promising strategy to tailor the spectral performance of the BDF by cryogenics.

## 2. Experimental schemes

The Bi-doped phosphosilicate fiber was fabricated by the conventional MCVD technique with *in-situ* solution doping method. The fiber under test (FUT) was drawn with a core diameter of 4  $\mu\text{m}$ , a cladding diameter of 125  $\mu\text{m}$ , and a cut-off wavelength of 0.94  $\mu\text{m}$ , the core compositions were estimated by the energy dispersive X-ray (EDX) analysis as [P]  $\sim 2.5$ , [Si]  $\sim 40$  at%, whereas the bismuth concentration is below the detection limit  $\sim 0.02$  at%. For all the fibers under test (FUTs) with different experiments, they were prepared with a “three-section” structure, namely, the two ends of a short piece of BEDF ( $\sim 5$  cm) were spliced with passive Hi-980 single-mode fibers ( $\lambda_c \sim 940$  nm, core diameter  $\sim 3.8$   $\mu\text{m}$ ) to ensure pump stability and minimize the modal interference. For spectral luminescence characterization (Fig. 1(a)), the FUT was spliced with the common port of the wavelength division multiplexer (WDM). The luminescence spectra were collected backward by an optical spectral analyzer (OSA, Agilent 86140B) and corrected for the insertion loss. The residual pump power was monitored by an optical power meter to evaluate the variation of pump absorption at different pump powers. To investigate the cooling effect on the gain performance, the counter-propagating measurement scheme was utilized (Fig. 1(b)). The on-off gain ( $g(\lambda)$ ) is defined as the ratio of the transmitted optical power with pump on ( $P_1$ ) and off ( $P_2$ ), defined as  $g(\lambda) = \frac{10}{L} \times \log(p_1 \times p_2)$ , where  $L$  is the length of BDF. For all experiments

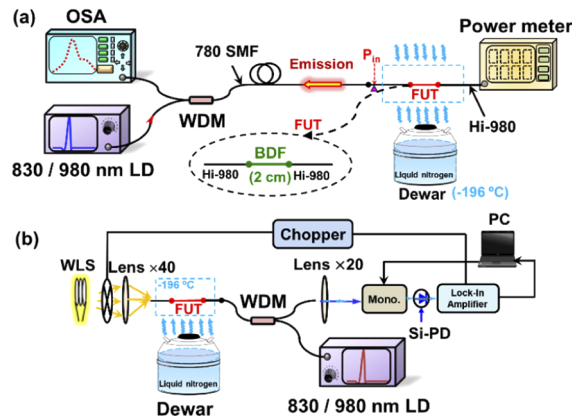


**Fig. 1.** (a) Schematic for backward luminescence measurement of the BDF under 830/980 nm laser pumping at RT and LNT. (b) On-off gain measurement scheme under 830/980 nm pumping at RT and LNT.

cooling in the liquid nitrogen environment, the FUT was fully immersed inside the bottom of the Dewar (~1 Liter) to ensure stable cryogenic temperature during the test process. The cooling time was varied from 5 to 10 minutes depending on the specific time required for data recording in each experiment.

### 3. Experimental results and discussion

Firstly, the small-signal absorption spectra of the FUT at RT and LNT were measured by the insertion method, as shown in Fig. 2(a). Several Bi-related absorption bands are observed, which are ascribed to two types of BACs: BAC-Si for 816 and 1400 nm [17,18], and BAC-P for 720 nm and a consecutive one from 900 to 1300 nm [19–21]. Upon cooling to LNT, the absorption bands of BACs feature negligible changes, except for the slight increase of the absorption band of BAC-P at 720 nm. In contrast, it is seen that the unsaturable loss level ( $\alpha_{\text{uns}}$ ) at 980 nm is decreased noticeably to 18 dB/m at LNT (Fig. 2(b)) without the change of the small-signal absorption ( $\alpha_{\text{tot}}$ ) at 980 nm. This indicates a higher pumping efficiency at 980 nm at LNT because the ratio of saturable absorption ( $\alpha_s = \alpha_{\text{tot}} - \alpha_{\text{uns}}$ ) has been increased [14,21]. The  $\alpha_{\text{uns}}$  contributing to the background loss is known to be related to the presence of the reduced form of bismuth (metallic, dimeric, clusters) during the fiber fabrication process, especially the preform collapse involving high-temperature annealing [22]. In our case, the  $\alpha_{\text{uns}}$  level is relatively high (75% of the  $\alpha_{\text{tot}}$  at 980 nm) due to the restricted and unsound fabrication conditions. For this reason, the true optical amplification and lasing are not achieved in our homemade BDFs. However, it doesn't affect the results of the whole study of the cooling effect on the optical properties of BAC-P and investigation of possible approaches for tuning spectral scheme in our homemade BDFs, which are our primary purposes.

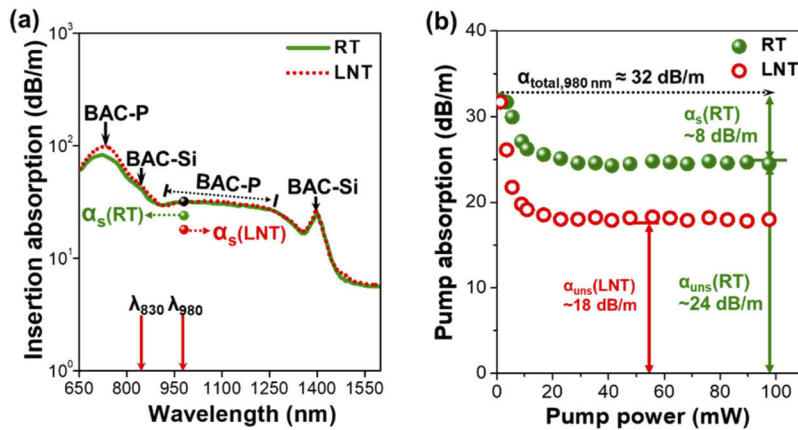


**Fig. 2.** (a) Small signal absorption spectra of the BDF at RT and LNT, with unsaturable loss levels indicated by points at 980 nm for RT and LNT. (b) Pump absorption at 980 nm versus pump power at RT and LNT.

To investigate the cooling effect on the spectral luminescence of BACs in BDFs, the backward pumping scheme was applied (Fig. 1(a)). Typical luminescence spectra in the near-IR range 900–1600 nm at RT and LNT under 830 nm pumping ( $P_{\text{in}} \sim 35$  mW) are illustrated in Figs. 3(a) and 3(b). As shown in Fig. 3(a), under 830 nm pumping at RT, a complex and broadband luminescence spectrum is observed. The well-known Gaussian decomposition method is applied for analyzing the overlapped luminescence bands, as reported in [23–25]. With the precise Gaussian decomposition ( $R^2 \sim 0.9996$ ), two predominant emission bands are distinguished, which are ascribed well-known BAC-P ( $\lambda \sim 1250$  nm,  $\Delta\lambda_{\text{FWHM}} \sim 285$  nm) and BAC-Si ( $\lambda \sim 1400$  nm,

$\Delta\lambda_{FWHM} \sim 145$  nm) [26,27]. In contrast, at LNT, the shape of luminescence bands features an intrinsic difference as compared to RT. It is revealed that there also exist two dominant emission bands attributed to BAC-P ( $\lambda \sim 1280$  nm,  $\Delta\lambda_{FWHM} \sim 270$  nm) and BAC-Si ( $\lambda \sim 1410$  nm,  $\Delta\lambda_{FWHM} \sim 80$  nm), respectively. Obviously, a noticeable red shift and narrowed bandwidth are observed for both BAC bands at a lower temperature. The wavelength shift is caused by the increased population residing in the lower levels of the upper manifold at LNT, resulting in the enhanced luminescence at longer wavelengths, while the narrowed bandwidth is caused by the weakening effect of homogeneous broadening [28]. However, it is found that the integral luminescence of BACs at LNT is enhanced significantly ( $\sim 1.68$  times), which is contributed by the steep rise of the luminescence of BAC-P at 1280 nm. Obviously, a low operating temperature results in the energy redistribution of BACs, with the enhancement of BAC-P's luminescence at the expense of BAC-Si. This may be explained by the slower interactive energy transfer process from BAC-P to BAC-Si due to the reduction of non-radiative transition probability at LNT [29].

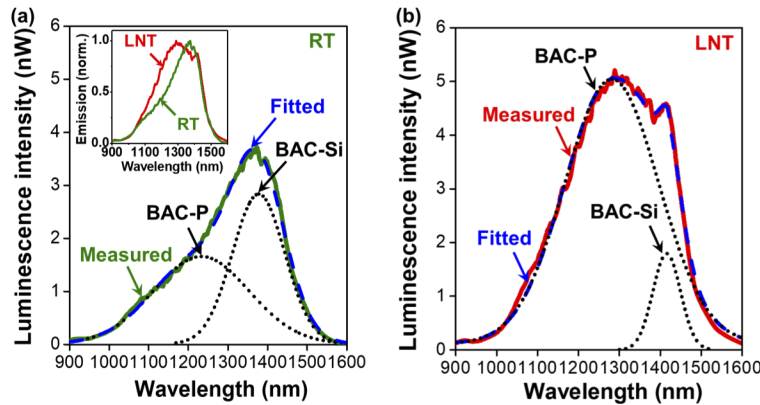


**Fig. 3.** NIR luminescence spectra of the BDF under 830 nm pumping ( $P_{in} \sim 35$  mW) at (a) RT and (b) LNT. Inset: Normalized luminescence spectra of the BDF under 830 nm pumping at RT and LNT.

The integral luminescence intensity of the BDF in the measured spectral range at both RT ( $I_{RT}$ ) and LNT ( $I_{LNT}$ ) as a function of 830 nm pump power was also measured, as shown in Fig. 4(a). It is seen that, with the increase of the pump power, the integrated luminescence of both BACs increases monotonically. Of note, it is found that, at all available pump powers, the luminescence intensity at LNT is  $\sim 1.7$  times stronger than that obtained at RT, indicating the predominance of BAC-P's luminescence over BAC-Si at a lower temperature. Moreover, the luminescence kinetics for BACs at different wavelengths were also measured at different temperatures under 830 nm pumping (Fig. 4(b)). It is seen that the luminescence decay at different wavelengths well fits a single exponential decline, and these BACs ( $\tau_{BAC-P} \sim 412$   $\mu$ s,  $\tau_{BAC-Si} \sim 616$   $\mu$ s at RT) are strongly distinguished by different lifetimes, indicating the independence of these BACs from each other.

Since we are of interest in the cooling effect on the luminescence properties of BAC-P, the 980 nm CW laser was then utilized to activate only BAC-P without the emergence of BAC-Si's luminescence at 1430 nm. Typical luminescence spectra of the BDF at RT and LNT under 980 nm pumping are depicted in Fig. 5. At RT, a broadband luminescence spectrum peaking at 1300 nm (BAC-P) is observed (Fig. 5(a)), with a dip at 1380 nm due to the  $OH^-$  overtones in the fiber. As the pump power increases, the luminescence intensity increases smoothly without the change of spectral shape. Similar behavior is also found at LNT (Fig. 5(b)).

Despite the smooth rise of the luminescence spectra with increasing pump power, it is found that the shape of the luminescence spectra obtained at LNT differs significantly from those obtained at RT, evidenced by a noticeable redshift of peak wavelength and remarkable enhancement in the

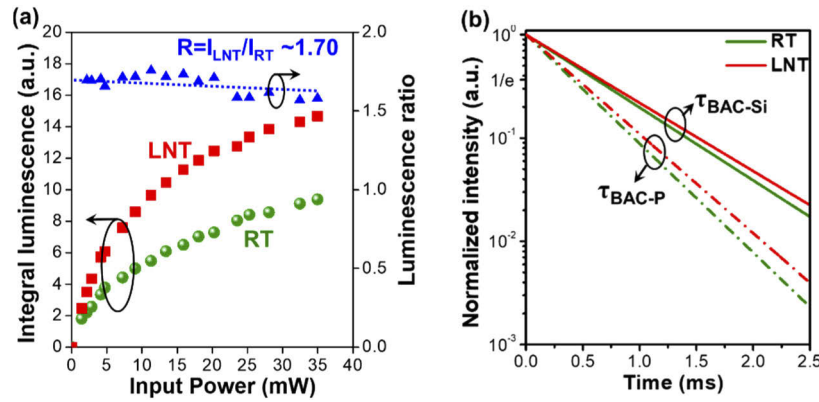


**Fig. 4.** (a) Integral NIR luminescence intensity of the BDF versus 830 nm input power at RT and LNT. (b) Luminescence decay at luminescence wavelengths of 1280 and 1410 nm at RT and LNT.

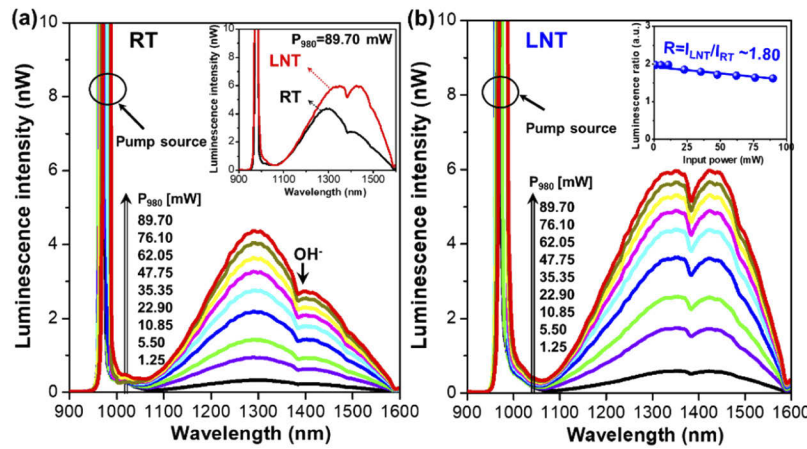


**Fig. 5.** Luminescence spectra versus pump power at (a) RT and (b) LNT. Inset of (a) compares the luminescence spectra at RT and LNT with the same pump power ( $P_{in} \sim 89.7$  mW). Inset of (b) depicts the integral luminescence intensity ratio of LNT to RT versus pump power.

spectral region 1400–1600 nm. It is found that the overall luminescence intensity is enhanced by  $\sim 1.8$  times for all pump powers at LNT. From the dramatic shape change of luminescence spectra, it is suggested that there should be more than one active component contributing to the enhanced NIR luminescence. Thus, Gaussian decomposition was applied to further analyze the distinct active components of the luminescence spectra, as depicted in Figs. 6(a) and 6(b). As seen in Fig. 6(a), (a) relatively weak but clear luminescence band peaking at 1470 nm is revealed with the extraction of Gaussian decomposition. This new emission band is overlapped with the well-known and dominant one peaking at 1300 nm (labeled as BAC-P1 [27,30]). Since the luminescence of BAC-Si at 1400 nm is absent at 980 nm excitation [31–33], it is reasonable to deduce that this additional emission band should also originate from the BAC coordinating with phosphorus (denoted as BAC-P2), but with a distinct local structural configuration from the dominant BAC-P1 at 1300 nm. To verify this point, the luminescence kinetics at these specific luminescence wavelengths were measured at both temperatures by using the time-resolved spectroscopic method described in [34], as plotted in the insets of Figs. 6(a) and 6(b). It is seen



that these two decay curves perfectly fit single exponential declines and are clearly distinguished by luminescence lifetimes. This strongly suggests the independence of luminescent sub-bands of BAC-P from each other under 980 nm pumping. As the temperature decreases to LNT (Fig. 6(b)), the luminescence intensity of BAC-P2 is enhanced significantly from 0.3 to 0.6, leading to a balanced and strengthened luminescence spectrum covering the whole spectral range. Based on the analysis of Gaussian fitting and luminescence kinetics, the possible low-lying energy levels of BACs-P are constructed with the 980 nm pumping (Fig. 6(c)). Evidently, a low temperature facilitates the optical transition of BAC-P2 in a longer wavelength range, resulting in higher luminescence efficiency at cryogenic temperatures.

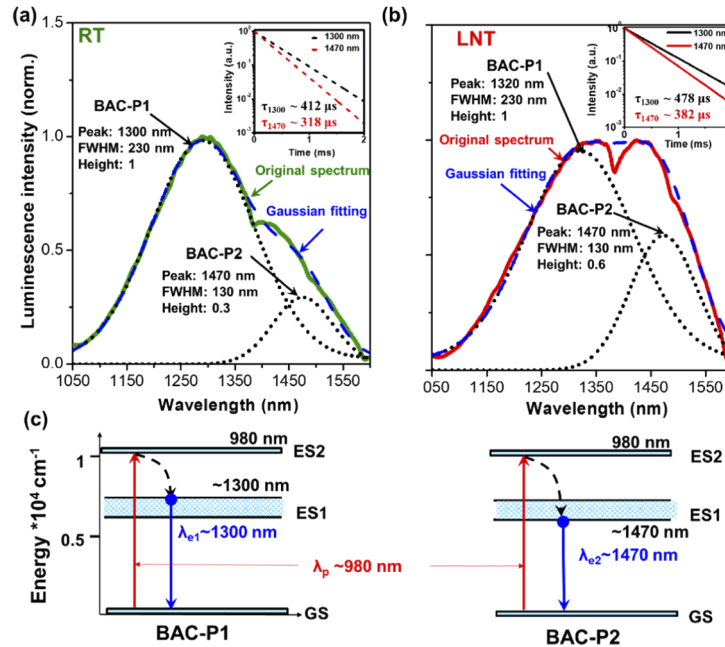


**Fig. 6.** Normalized luminescence spectra with Gaussian fitting of the BDF at (a) RT and (b) LNT under 980 nm pumping ( $P_{in} \sim 89.70$  mW). Inset: Luminescence decay at 1300 and 1470 nm under excitation at 980 nm at RT and LNT. (c) Possible lower-lying energy levels of BAC-P1 and BAC-P2 under excitation at 980 nm.

In addition to the luminescence characterization, on-off gain measurements were also carried out to investigate the influence of fiber temperature on the optical on-off gain performance. The counter-propagation measurement scheme was utilized under the excitation at 830 and 980 nm, as illustrated in Fig. 1(b). The fiber was selected to ensure pump saturation over the full length ( $\sim 5$  cm) for the excited state absorption (ESA) or optical gain occurring at the metastable levels. Typical NIR on-off gain spectra of the BDF at RT and LNT under excitation at 830 and 980 nm are illustrated in Figs. 7(a) and 7(b).

Upon 830 nm pumping (Fig. 7(a)), an obvious on-off gain band peaking around 1400 nm is observed, which is ascribed to the stimulated amplification of BAC-Si [18,32], whereas an intense ESA band is revealed in the range 950-1350 nm. The broad ESA band peaking around 1000 nm is associated with BAC-P since no apparent ESA is found for BAC-Si in Bi-doped pure silicate fiber [35]. Upon cooling at LNT, the gain band at 1420 nm increase slightly ( $\sim 2.5$  dB/m) with narrower bandwidth, whereas the ESA of BAC-P is aggravated noticeably. This coincides with the luminescence results upon 830 nm excitation since more BAC-P sites are populated for the subsequent transition to the higher-lying levels at LNT. In contrast, under excitation

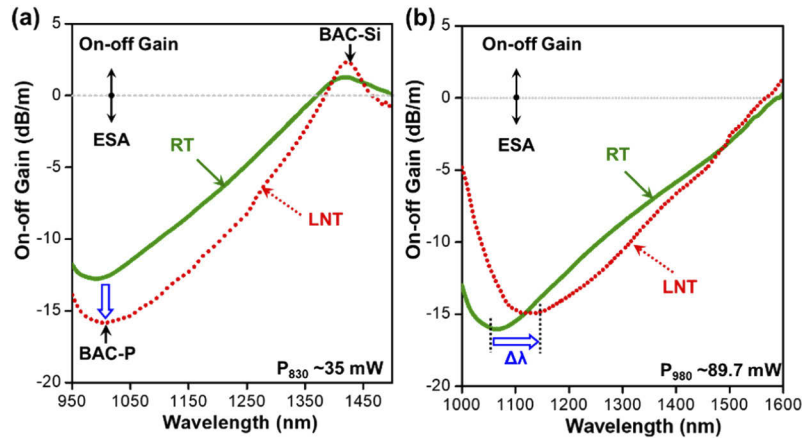


**Fig. 7.** On-off gain spectra of the BDF at RT and LNT under (a) 830 nm pumping ( $P_{in} \sim 35$  mW) and (b) 980 nm pumping ( $P_{in} \sim 89.7$  mW).

at 980 nm, a broad ESA spectrum without any gain band is observed throughout the whole region of 1000-1600 nm, which is caused by the dominant pump and signal ESA occurred at BAC-P. Different from the results obtained with 830 nm excitation, the ESA spectrum features a noticeable redshift ( $\Delta\lambda \sim 50$  nm) and bandwidth broadening in the spectral range 1100-1300 nm at LNT. Clearly, the spectral change of the ESA spectrum at LNT should arise from the aggravated ESA from BAC-P2 at a longer wavelength, which is in good agreement with the shape change of luminescence under 980 nm pumping. However, as mentioned, since the unsaturable loss level is fairly high at the pumping wavelength, the true optical gain is not achieved in our homemade BDFs. Therefore, to fully demonstrate the benefits of cooling on the BDF-based devices, further research of the change of net gain of BAC-P at cryogenic temperatures in BDFs with lower unsaturable loss levels are required, along with the optimization of the pumping wavelength.

At last, the photoinduced effect (photobleaching) on the luminescence of BAC-P is also explored at RT and LNT to potentially obtain new knowledge on the nature of BAC-P. The measurement setup was similar to the one described in [31]. In fact, the photobleaching effect of BACs has been reported repeatedly in a few papers [30,36,37], leading to the destruction of NIR luminescence for different types of BACs. Similar results have been obtained with photobleaching of BAC-P under irradiation at various wavelengths (Fig. 8(a)). It is seen that the degradation of luminescence becomes more intense with the increase of photon energy and takes place for all available wavelengths regardless of the resonant transitions of BAC-P. This strongly suggests the structure similarity between BAC-P and other types of BACs (BAC-Si and BAC-Ge) [30,36]. The bleaching of BAC-P should be photoionization of phosphor-related defects forming BAC-P.

However, when the fiber is irradiated under 532 nm irradiation ( $I \sim 0.18$  MW/cm<sup>2</sup>) at LNT, A noticeable luminescence enhancement ( $\sim 10\%$ ), instead of degradation, is observed over the spectral range 1000-1600 nm after 1 h irradiation (Fig. 8(b)). This may be explained by the fact that the photoionization process becomes slower at a decreased temperature [38], which restrains the destruction of BAC-P at cryogenic temperatures, and the bleaching effect of BAC-P is already relatively weak at RT ( $\sim 10\%$ ). On the other hand, it is possible that laser irradiation at 532 nm under the cryogenic environment supports the growth of BAC-P's concentration, which in turn facilitates the luminescence in the spectral range 1100-1600 nm. It should be noted that laser irradiation luminescence enhancement has also been observed in Bi-doped fibers with other hosts [13]. Still, further research in this direction is required.

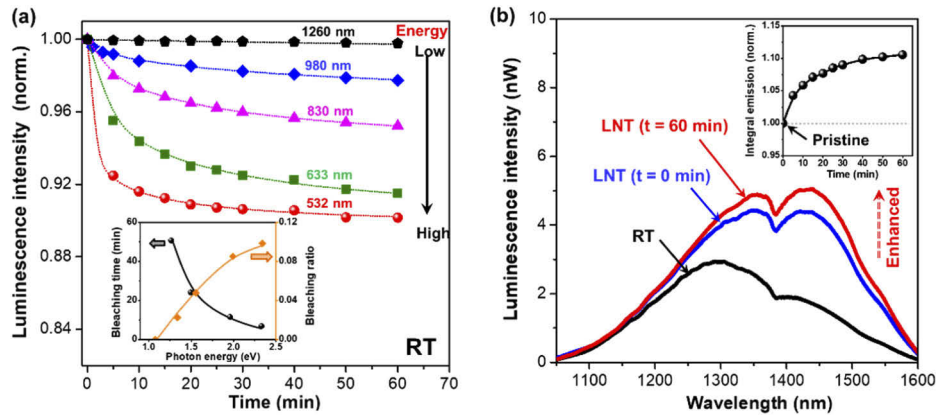


**Fig. 8.** (a) Evolution of the luminescence intensity at 1300 nm (BAC-P) under irradiation at various wavelengths. Inset: characteristic bleaching time and bleaching ratio as a function of photon energy. (b) Luminescence spectra of BDF at RT, LNT ( $t=0$  min), and LNT ( $t=60$  min after 532 nm irradiation). Inset: temporal dependence of integral luminescence on the exposition time at LNT.

#### 4. Conclusion

In conclusion, for the first time, the influence of cooling on the spectroscopic properties of Bi-doped phosphosilicate fibers has been systematically investigated. It is found that cooling at LNT can efficiently suppress the unsaturable absorption level without the change of the absorption bands of BACs. Moreover, it is revealed that the NIR luminescence of Bi-doped phosphosilicate fiber at 1300 nm is increased notably ( $\sim 2$  times) at LNT under either 830 or 980 nm pumping, contributed by the enhancement of BAC-P's luminescence. Specifically, the luminescence sub-band of BAC-P emitting around 1470 nm is revealed under 980 nm pumping, evidenced by the distinct lifetime from the dominant one peaking at 1300 nm. In addition, the spectral change of on-off gain at LNT is investigated, and the experimental data is in good agreement with the luminescence performance of BAC-P. Furthermore, the NIR luminescence enhancement ( $\sim 1.1$  times) is achieved upon 1 h 532 nm laser irradiation at LNT. It is believed that this detailed study allows for insights into the temperature-related spectral properties of BACs and provide new information on the unique nature of BAC-P and operating conditions of BDFs with  $\text{P}_2\text{O}_5$ - $\text{SiO}_2$  host in the low-temperature range, which in turn provides a promising strategy to tailor the spectral performance of the BDF by cryogenics.

#### Funding

National Key R and D program (2018YFB1800902); National Natural Science Foundation of China (61520106014, 61675032); Science and Technology Commission of Shanghai Municipality (SKLSFO2018-02); Overseas Expertise Introduction Project for Discipline Innovation (B18005).

#### Disclosures

The authors declare no conflicts of interest.

#### References

1. C. J. Koester and E. Snitzer, "Amplification in a fiber laser," *Appl. Opt.* **3**(10), 1182–1186 (1964).
2. S. V. Firstov, S. V. Alyshev, K. E. Riumkin, A. M. Khagai, A. V. Kharakhordin, M. A. Melkumov, and E. M. Dianov, "Laser-active fibers doped with bismuth for a wavelength region of 1.6–1.8  $\mu\text{m}$ ," *IEEE J. Sel. Top. Quantum Electron.* **24**(5), 1–15 (2018).



3. I. A. Bufetov, M. A. Melkumov, S. V. Firstov, K. E. Riumkin, A. V. Shubin, V. F. Khopin, A. N. Guryanov, and E. M. Dianov, "Bi-Doped Optical Fibers and Fiber Lasers," *IEEE J. Sel. Top. Quantum Electron.* **20**(5), 111–125 (2014).
4. N. K. Thipparapu, A. A. Umnikov, P. Barua, and J. K. Sahu, "Bi-doped fiber amplifier with a flat gain of 25 dB operating in the wavelength band 1320–1360 nm," *Opt. Lett.* **41**(7), 1518–1521 (2016).
5. Z. M. Sathi, J. Zhang, Y. Luo, J. Canning, and G. D. Peng, "Improving broadband emission within Bi/Er doped silicate fibres with Yb co-doping," *Opt. Mater. Express* **5**(10), 2096 (2015).
6. J. Zhang, Z. M. Sathi, Y. Luo, J. Canning, and G.-D. Peng, "Toward an ultra-broadband emission source based on the bismuth and erbium co-doped optical fiber and a single 830 nm laser diode pump," *Opt. Express* **21**(6), 7786–7792 (2013).
7. S. V. Firstov, S. V. Alyshev, K. E. Riumkin, V. F. Khopin, A. N. Guryanov, M. A. Melkumov, and E. M. Dianov, "A 23-dB bismuth-doped optical fiber amplifier for a 1700-nm band," *Sci. Rep.* **6**(1), 28939 (2016).
8. S. V. Firstov, S. V. Alyshev, V. F. Khopin, A. V. Kharakhordin, A. S. Lobanov, E. G. Firstova, K. E. Riumkin, A. M. Khagai, M. A. Melkumov, and A. N. Guryanov, "Effect of heat treatment parameters on the optical properties of bismuth-doped GeO<sub>2</sub>: SiO<sub>2</sub> glass fibers," *Opt. Mater. Express* **9**(5), 2165–2174 (2019).
9. Q. C. Zhao, J. Z. Zhang, D. Sporea, Y. H. Luo, J. X. Wen, and G. D. Peng, "Gamma radiation and thermal-induced effects on the spectral performance of BACs in Bi/Er codoped aluminosilicate fibers," *Opt. Express* **27**(7), 9955–9964 (2019).
10. S. V. Firstov, V. F. Khopin, S. V. Alyshev, E. G. Firstova, K. E. Riumkin, M. A. Melkumov, A. M. Khagai, P. F. Kashaykin, A. N. Guryanov, and E. M. Dianov, "Effect of gamma-irradiation on the optical properties of bismuth-doped germanosilicate fibers," *Opt. Mater. Express* **6**(10), 3303–3308 (2016).
11. J. Wen, W. Liu, Y. Dong, Y. Luo, G.-d. Peng, N. Chen, F. Pang, Z. Chen, and T. Wang, "Radiation-induced photoluminescence enhancement of Bi/Al-codoped silica optical fibers via atomic layer deposition," *Opt. Express* **23**(22), 29004–29013 (2015).
12. A. P. Bazakutsa, O. V. Butov, and K. M. Golant, "Influence of hydrogen loading on active fibers," in *2013 Optical Fiber Communication Conference and Exposition and the National Fiber Optic Engineers Conference (OFC/NFOEC)*, 2013), 1–3 (2013).
13. C. Ban, L. I. Bulatov, V. V. Dvoyrin, V. M. Mashinsky, H. G. Limberger, and E. M. Dianov, "Infrared luminescence enhancement by UV-irradiation of H<sub>2</sub>-loaded Bi-Al-doped fiber," in *2009 35th European Conference on Optical Communication*, 2009), 1–2 (2009).
14. S. Wei, Y. Luo, D. Fan, G. Xiao, Y. Chu, B. Zhang, Y. Tian, M. Talal, M. Lancry, and G.-D. Peng, "BAC activation by thermal quenching in bismuth/erbium codoped fiber," *Opt. Lett.* **44**(7), 1872–1875 (2019).
15. Q. Zhao, Y. Luo, Q. Hao, and G.-D. Peng, "Effect of thermal treatment parameters on the spectral characteristics of BAC-Al in bismuth/erbium-codoped aluminosilicate fibers," *Opt. Lett.* **44**(18), 4594–4597 (2019).
16. Q. Zhao, Q. Hao, Y. Luo, and G.-D. J. O. L. Peng, "Thermal-induced luminescence enhancement of BAC-P in bismuth-doped phosphogermanosilicate fibers," *Opt. Lett.* **45**(5), 1152–1155 (2020).
17. I. A. Bufetov, S. L. Semenov, V. V. Vel'miskin, S. V. Firstov, G. A. Bufetova, and E. M. Dianov, "Optical properties of active bismuth centres in silica fibres containing no other dopants," *Quantum Electron.* **40**(7), 639–641 (2010).
18. I. A. Bufetov, M. A. Melkumov, S. V. Firstov, A. V. Shubin, S. L. Semenov, V. V. Vel'miskin, A. E. Levchenko, E. G. Firstova, and E. M. Dianov, "Optical gain and laser generation in bismuth-doped silica fibers free of other dopants," *Opt. Lett.* **36**(2), 166–168 (2011).
19. S. Firstov, I. Bufetov, V. Khopin, A. Shubin, A. Smirnov, L. Iskhakova, N. Vechkanov, A. Guryanov, and E. Dianov, "2 W bismuth doped fiber lasers in the wavelength range 1300–1500 nm and variation of Bi-doped fiber parameters with core composition," *Laser Phys. Lett.* **6**(9), 665–670 (2009).
20. I. A. Bufetov, S. V. Firstov, V. F. Khopin, O. I. Medvedkov, A. N. Guryanov, and E. M. Dianov, "Bi-doped fiber lasers and amplifiers for a spectral region of 1300–1470 nm," *Opt. Lett.* **33**(19), 2227–2229 (2008).
21. I. A. Bufetov and E. M. Dianov, "Bi-doped fiber lasers," *Laser Phys. Lett.* **6**(7), 487–504 (2009).
22. A. S. Zlenko, V. M. Mashinsky, L. D. Iskhakova, S. L. Semjonov, V. V. Koltashev, N. M. Karatun, and E. M. Dianov, "Mechanisms of optical losses in Bi: SiO<sub>2</sub> glass fibers," *Opt. Express* **20**(21), 23186–23200 (2012).
23. L. I. Bulatov, V. M. Mashinskii, V. V. Dvoirin, E. F. Kustov, and E. M. Dianov, "Luminescent properties of bismuth centres in aluminosilicate optical fibres," *Quantum Electron.* **40**(2), 153–159 (2010).
24. I. Razdobreev, H. El Hamzaoui, V. Y. Ivanov, E. F. Kustov, B. Capoen, and M. Bouazaoui, "Optical spectroscopy of bismuth-doped pure silica fiber preform," *Opt. Lett.* **35**(9), 1341–1343 (2010).
25. E. M. Dianov, "Bismuth-doped optical fibers: a challenging active medium for near-IR lasers and optical amplifiers," *Light: Sci. Appl.* **1**(5), e12 (2012).
26. S. V. Firstov, V. F. Khopin, I. A. Bufetov, E. G. Firstova, A. N. Guryanov, and E. M. Dianov, "Combined excitation-emission spectroscopy of bismuth active centers in optical fibers," *Opt. Express* **19**(20), 19551–19561 (2011).
27. E. G. Firstova, I. A. Bufetov, V. F. Khopin, V. V. Vel'miskin, S. V. Firstov, G. A. Bufetova, K. N. Nishchev, A. N. Guryanov, and E. M. Dianov, "Luminescence properties of IR-emitting bismuth centres in SiO<sub>2</sub>-based glasses in the UV to near-IR spectral region," *Quantum Electron.* **45**(1), 59–65 (2015).
28. C. A. Millar, T. J. Whitley, and S. C. Fleming, "Thermal-properties of an erbium-doped fiber amplifier," *IEEE Proc.-J: Optoelectron.* **137**(3), 155–162 (1990).

29. B. Yan, Y. Luo, A. Zareanborji, G. Xiao, G.-D. Peng, and J. Wen, "Performance comparison of bismuth/erbium co-doped optical fibre by 830 nm and 980 nm pumping," *J. Opt.* **18**(10), 105705 (2016).
30. S. V. Firstov, S. V. Alyshev, A. V. Kharakhordin, K. E. Riumkin, and E. M. Dianov, "Laser-induced bleaching and thermo-stimulated recovery of luminescent centers in bismuth-doped optical fibers," *Opt. Mater. Express* **7**(9), 3422–3432 (2017).
31. Q. Zhao, Y. Luo, Y. Tian, and G.-D. Peng, "Pump wavelength dependence and thermal effect of photobleaching of BAC-Al in bismuth/erbium codoped aluminosilicate fibers," *Opt. Lett.* **43**(19), 4739–4742 (2018).
32. Q. Zhao, J. Zhang, Y. Luo, J. Wen, and G.-D. Peng, "Energy transfer enhanced near-infrared spectral performance in bismuth/erbium codoped aluminosilicate fibers for broadband application," *Opt. Express* **26**(14), 17889–17898 (2018).
33. S. V. Firstov, S. V. Alyshev, E. G. Firstova, M. A. Melkumov, A. M. Kheday, V. F. Khopin, A. N. Guryanov, and E. M. Dianov, "Dependence of the photobleaching on laser radiation wavelength in bismuth-doped germanosilicate fibers," *J. Lumin.* **182**(1), 87–90 (2017).
34. A. Zareanborji, H. Yang, G. E. Town, Y. Luo, and G.-D. Peng, "Simple and accurate fluorescence lifetime measurement scheme using traditional time-domain spectroscopy and modern digital signal processing," *J. Lightwave Technol.* **34**(21), 5033–5043 (2016).
35. K. E. Riumkin, M. A. Melkumov, I. A. Varfolomeev, A. V. Shubin, I. A. Bufetov, S. V. Firstov, V. F. Khopin, A. A. Umnikov, A. N. Guryanov, and E. M. Dianov, "Excited-state absorption in various bismuth-doped fibers," *Opt. Lett.* **39**(8), 2503–2506 (2014).
36. S. Firstov, S. Alyshev, V. Khopin, M. Melkumov, A. Guryanov, and E. Dianov, "Photobleaching effect in bismuth-doped germanosilicate fibers," *Opt. Express* **23**(15), 19226–19233 (2015).
37. S. Firstov, E. Firstova, S. Alyshev, V. Khopin, K. Riumkin, M. Melkumov, A. Guryanov, and E. Dianov, "Recovery of IR luminescence in photobleached bismuth-doped fibers by thermal annealing," *Laser Phys.* **26**(8), 084007 (2016).
38. H. Hosono, Y. Abe, D. L. Kinser, R. A. Weeks, K. Muta, and H. J. P. R. B. Kawazoe, "Nature and origin of the 5-eV band in SiO<sub>2</sub>: GeO<sub>2</sub> glasses," *Phys. Rev. B* **46**(18), 11445–11451 (1992).